ELSEVIER

Ceramics International 32 (2006) 623–632

CERAMICS INTERNATIONAL

www.elsevier.com/locate/ceramint

Sol–gel synthesis of lithium aluminum silicate powders: The effect of silica source

Minati Chatterjee, Milan Kanti Naskar *

Sol–Gel Division, Central Glass and Ceramic Research Institute, 196 Raja S.C. Mullick Road, Jadavpur, Kolkata 700 032, India

Received 2 February 2005; received in revised form 21 March 2005; accepted 21 March 2005
Available online 5 July 2005

Abstract

Lithium aluminum silicate (LAS) powders were synthesized through sol–gel technique by using three different sources of silica, i.e., TEOS, fumed silica and rice husk ash and their effects on the characteristics of the powders were studied. The gel and oxide powders were characterized by thermogravimetry (TG), differential thermal analysis (DTA), X-ray diffraction (XRD), Fourier transformed infrared (FTIR) spectroscopy and scanning electron microscopy (SEM). DTA and XRD results showed that the crystallization of β-eucryptite and β-spodumene started at about 700 °C for TEOS and fumed silica sources while the same crystallized at about 785 °C for rice husk ash source. FTIR study confirmed the presence of nonbridging oxygen in AlO_6 octahedra for β-eucryptite prepared from TEOS source calcined at 400–600 °C and the same was found for fumed silica and rice husk ash sources calcined at 400–1000 °C. SEM showed the formation of cobble-stone-like morphology of β-spodumene obtained from three different sources of silica.

Keywords: A. Sol–gel process; A. Powder: chemical preparation; D. Glass ceramics; Crystallization

1. Introduction

Synthesis of lithium aluminum silicate (LAS) glass-ceramics, one of the most important glass-ceramic system, has attracted a great attention over the past several years, because of its low and even negative thermal expansion coefficient as well as excellent thermal and chemical durability [1–3]. They are used in industry as furnace materials and as gas turbine heat exchangers where the dimensional stability and ability to resist thermal shock are necessary. Some other widespread applications of LAS glass-ceramics are telescope mirror blanks, ring-laser gyroscope, optically stable platforms, stove windows, cookware and cook top panels [2]. The dominant crystalline phase in LAS glass-ceramics is either β-eucryptite ($Li_2O{\cdot}Al_2O_3{\cdot}2SiO_2$) or β-spodumene ($Li_2O{\cdot}Al_2O_3{\cdot}4SiO_2$) solid solution. There are many conventional methods in synthesizing of LAS powders. The β-spodumene, commercially available glass-ceramics, are prepared mainly by the recrystallization of solidified glass melt, but there arise a problem of its sintering without proper sintering aid. The incorporation of a sintering aid results in a large thermal expansion coefficient [4]. Therefore, the preparation of homogeneous and fine β-spodumene and eucryptite powders is becoming an important technical objective.

In recent times sol–gel methods [3,5–7] have been considered promising for preparing ultrafine, high purity, single and multicomponent oxide glasses and ceramic composites with the advantages of high purity, lower sintering temperature, a high degree of homogeneity, high yield, small processing time, cost effectiveness and environment friendly [8,9]. Most of the sol–gel methods [10–13] of preparing LAS glass-ceramics are alkoxide based, and therefore, control of hydrolysis and condensation reaction of different metal alkoxides is becoming difficult towards the formation of a common network in which the various metal ions are included. Several attempts have been carried out including matching of hydrolysis rates by chemical modifications with chelating ligands, synthesis of

* Corresponding author. Tel.: +91 33 2483 8086; fax: +91 33 2473 0957.
E-mail address: milan@cgcri.res.in (M.K. Naskar).

0272-8842/$30.00
doi:10.1016/j.ceramint.2005.03.033

multicomponent alkoxides, or partial prehydrolysis of alkoxides [14–17]. However, all the approaches are very complex in nature and time consuming too.

In the present investigation, lithium aluminum silicate (LAS) powders in the form of β-eucryptite and β-spodumene were synthesized following the sol–gel method starting with aquo-based inorganic metal salt solutions [7,8]. In this study three different silica source materials namely, tetraethyl orthosilicate (TEOS), fumed silica and rice husk ash were used in synthesizing LAS powders following the same experimental procedure. The main objective of the present work is to study the effect of silica sources on the characteristics of the LAS powders. With this view, the prepared powders obtained from different silica sources were characterized by differential thermal analysis (DTA), thermogravimetric (TG) analysis, X-ray diffraction (XRD), Fourier transformed infrared (FTIR) spectroscopy and scanning electron microscopy (SEM).

2. Experimental procedure

2.1. Preparation of sols, gels and oxide powders

Fig. 1 presents the flow diagram for the preparation of lithium aluminum silicate powders using different sources, i.e., TEOS, fumed silica and rice husk ash. For the preparation of sols in the tri-component system of Li_2O–Al_2O_3–SiO_2, two steps were followed: (i) preparation of bi-component sol of lithia–alumina with their stoichiometric compositions and (ii) preparation of tri-component sol of lithia–alumina–silica with their stoichiometric compositions by the addition of different silica sources to the bi-component sol prepared as in (i) above.

In the first step, the precursor materials for the preparation of lithia–alumina (1:1 mole ratio) sol were lithium nitrate, $LiNO_3$ (A.R., Merck India, purity >99%) and hydrated aluminum nitrate, $Al(NO_3)_3{\cdot}9H_2O$ (A.R., Merck India, purity >99%). An aqueous alumina sol was prepared by dissolving calculated quantity of $Al(NO_3)_3{\cdot}9H_2O$ in deionized water to make 1 M solution followed by allowing adequate polymerization of the $[Al(H_2O)_6^{3+}]$ present at 80 ± 1 °C under controlled condition, i.e., by dropwise addition of concentrated ammonia solution (25 wt.%, G.R., Merck, India) up to pH of about 3 under vigorous stirring in a covered container [7–9]. The viscosity of the resulting sol increased with increasing time of heating. The heating was continued until the final viscosity of the transparent sol was determined to be 15 ± 1 mPa s. The pH of the sols was measured with a Jencons pH meter (Model 3030) while the viscosity values were recorded using a Brookfield viscometer (Model LVTDV-II). For the preparation of the bi-component sol, calculated quantity of $LiNO_3$, corresponding to the equivalent amount of Li_2O was then added to the alumina sol under stirring, maintaining pH ~ 3.3 to obtain a clear sol of alumina–lithia.

In the second step, calculated quantities of TEOS (Fluka Chemica, Purum grade, ≥98%), fumed silica (Cab-O-Sil,

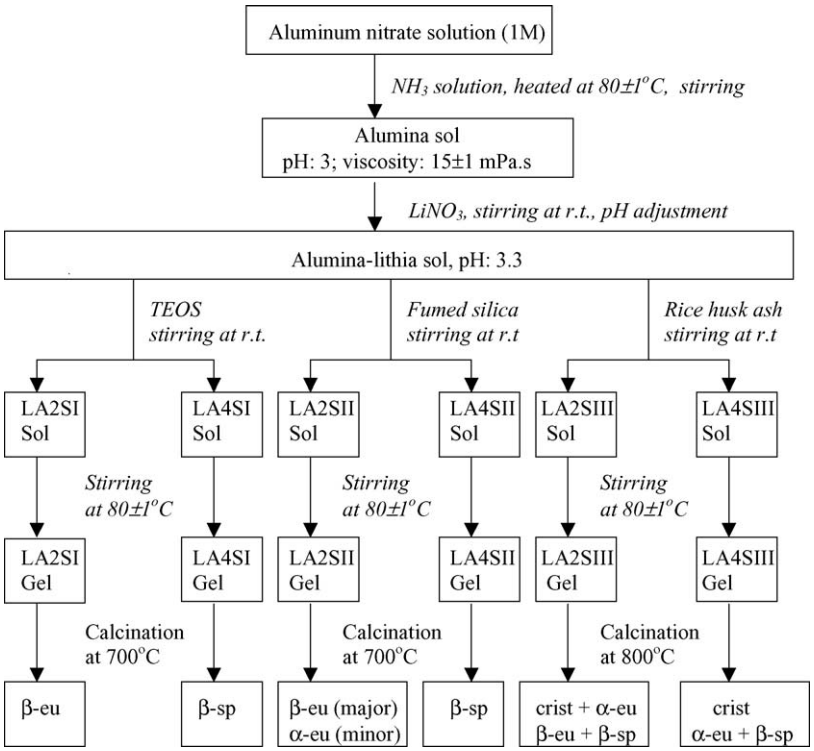

Fig. 1. A flow diagram for the synthesis of LAS powders from different silica sources. α-eu: α-eucryptite, β-eu: β-eucryptite, β-sp: β-spodumene, crist: cristobalite.

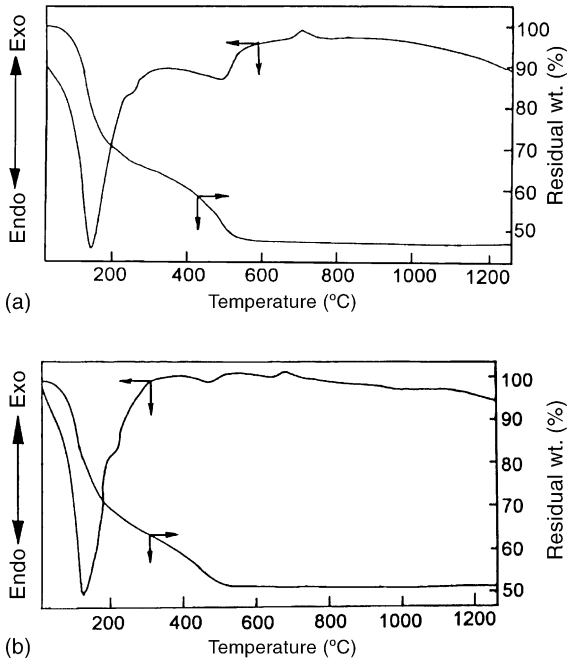

Fig. 2. DTA and TG of (a) LA2SI powders and (b) LA4SI powders obtained from TEOS.

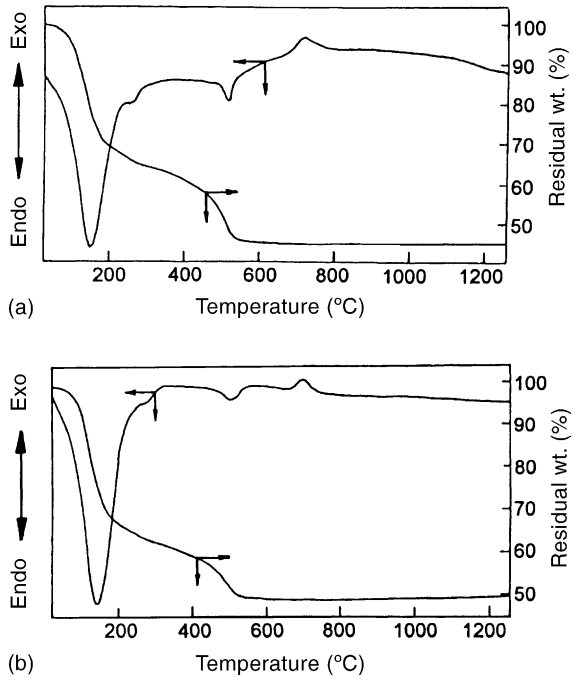

Fig. 3. DTA and TG of (a) LA2SII powders and (b) LA4SII powders obtained from fumed silica.

Cabot Corporation, 95.84 wt.% SiO_2) and rice husk ash (crystalline form: cristobalite, composition (wt.%): SiO_2 (90.23%), TiO_2 (0.13%), Al_2O_3 (1.07%), Fe_2O_3 (0.27%), CaO (0.39%), MgO (0.18%), K_2O (1.36%), P_2O_5 (2.38%), L.O.I. (3.99%)) were added under stirring at RT to the bi-component sols to prepare tri-component sols of lithia–alumina–silica. Before using, the ash was ground to make −300 mesh powder. For different stoichiometric composition of Li_2O–Al_2O_3–SiO_2, two sets of sol, namely LA2S ($Li_2O{\cdot}Al_2O_3{\cdot}2SiO_2$) and LA4S ($Li_2O{\cdot}Al_2O_3{\cdot}4SiO_2$) were thus prepared; and for each source of silica, the sols were designated as LA2SI and LA4SI for TEOS, LA2SII and LA4SII for fumed silica and LA2SIII and LA4SIII for rice husk ash sources. The sols were continuously heated at 80 ± 1 °C under stirring to obtain the corresponding gel powder. The agglomerated gels were ground to make −300 mesh powders. The gel powders thus obtained were subjected to calcinations from 400 °C to 1000 °C each, with a heating rate of 3.3 °C/min and with a dwell time of 1 h under a programmable furnace in static air condition to obtain the desired oxide powders.

2.2. Characterization of gels and oxide powders

The gel powders were characterized by differential thermal analysis (DTA) and thermogravimetry (TG) (Netzsch STA 409c) from 30 °C to 1200 °C in Ar atmosphere at the heating rate of 10 °C/min. Crystalline phases of the calcined powders developed at different temperatures were examined by X-ray diffraction (XRD) (Philips PW-1730 with Ni-filtered Cu Kα radiation). The IR vibrational spectroscopy of different gel and calcined samples was performed with Fourier transform infrared (FTIR) study (Nicolet 5 PC) in the wavenumber range 4000–400 cm^{-1} using 4.0 cm^{-1} resolution. The microstructures of the calcined (1000 °C) powders were observed with the help of scanning electron microscopy (SEM) (Cambridge Stereoscan S 430i).

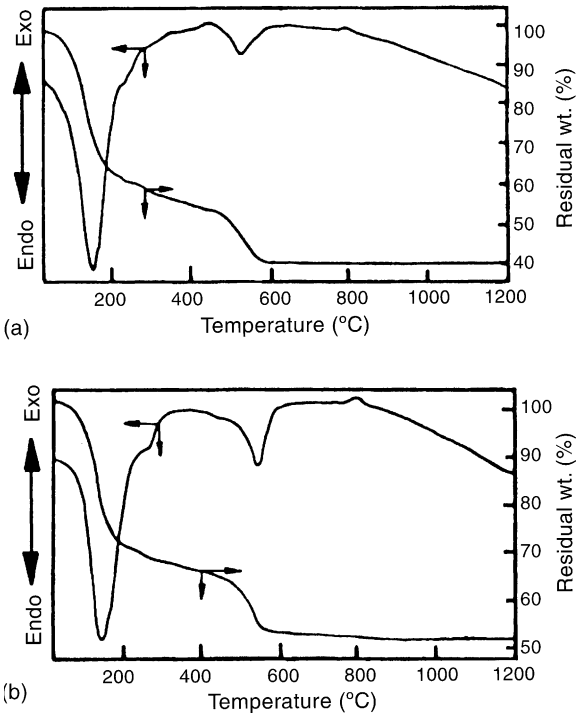

Fig. 4. DTA and TG of (a) LA2SIII powders and (b) LA4SIII powders obtained from rice husk ash.

3. Results and discussion

3.1. Thermal analysis by DTA and TG

DTA and TG curves for the gel samples, LA2SI, LA4SI, LA2SII, LA4SII, LA2SIII and LA4SIII are shown in Figs. 2a, b, 3a, b and 4a, b, respectively. For the gel samples, LA2SI and LA4SI obtained from TEOS, Fig. 2a and b, respectively, show strong broad endothermic peak at 145 °C for the former and that at 125 °C for the latter. Fig. 2a and b also reveal another endothermic peak at around 250 °C for both the samples LA2SI and LA4SI. In the corresponding TG curves (Fig. 2a and b), a total weight loss of about 36% was observed in the temperature region 30–300 °C for the samples LA2SI and LA4SI. A broad endothermic peak was also found at around 480 °C for both the samples LA2SI and LA4SI accompanying a weight loss of 17% for the former and that of 13% for the latter in the temperature region 300–600 °C of the TG curves (Fig. 2a and b). An exothermic peak at 700 °C was noticed for the sample LA2SI (Fig. 2a) while the same was observed at 690 °C for the sample LA4SI (Fig. 2b). In the temperature region 600–1200 °C there appeared practically no weight loss in the corresponding TG curves (Fig. 2a and b).

For the gel samples, LA2SII and LA4SII obtained from fumed silica, Fig. 3a and b, respectively, depict strong broad endothermic peaks at 150 °C for the former and that at 140 °C for the latter. Two other endothermic peaks were found at 260 °C for LA2SII (Fig. 3a) and at 255 °C for LA4SII (Fig. 3b). In the TG curves (Fig. 3a and b), a total weight loss of 36.5% for the sample LA2SII (Fig. 3a) and that of 38% for the sample LA4SII (Fig. 3b) were noticed in the temperature region 30–300 °C. Fig. 3a and b also show another endothermic peak at 515 °C for LA2SII and that at 500 °C for LA4SII, respectively. In the temperature region 300–600 °C, the weight loses of 15.7% and 11% were recorded for the sample LA2SII (Fig. 3a) and LA4SII (Fig. 3b), respectively. The exothermic peaks were appeared at 705 °C and 696 °C for the sample LA2SII (Fig. 3a) and LA4SII (Fig. 3b), respectively. In the corresponding TG curves (Fig. 3a and b), no weight loss was found in the temperature region 600–1200 °C.

DTA curve for the gel sample, LA2SIII obtained from rice husk ash shows a broad endothermic peak at 147 °C and another small endothermic peak at 275 °C (Fig. 4a); the corresponding endothermic peak temperatures for the gel sample, LA4SIII obtained from the same source were observed at 145 °C and 270 °C (Fig. 4b). From the TG

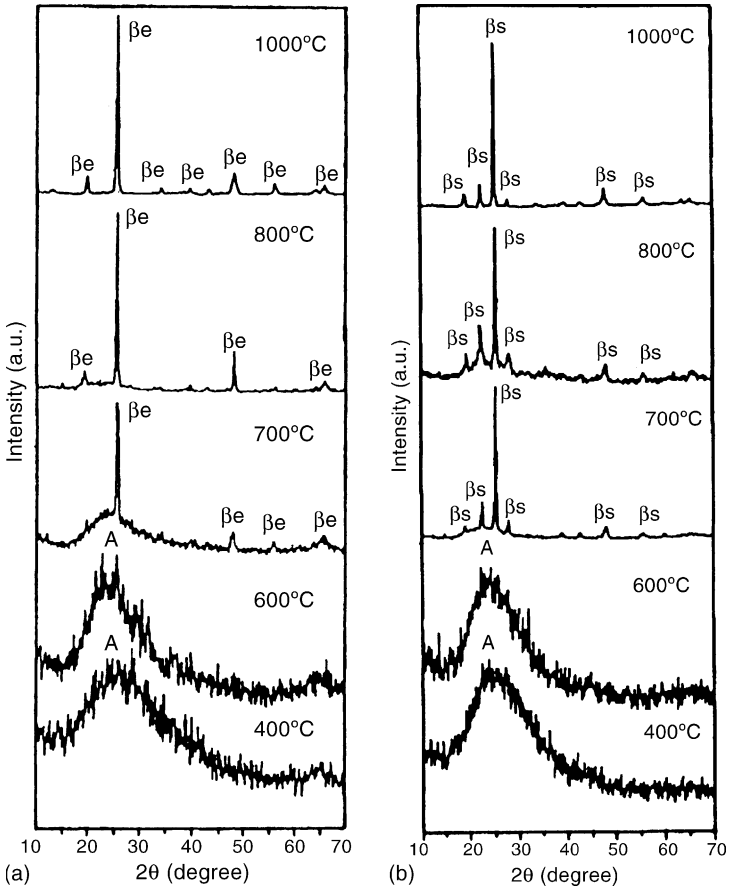

Fig. 5. (a) XRD patterns of LA2SI powders obtained from TEOS and calcined at 400–1000 °C. *Note*: Dwell time: 1 h at each temperature. A: amorphous and βe: β-eucryptite. (b) XRD patterns of LA4SI powders obtained from TEOS and calcined at 400–1000 °C. *Note*: Dwell time: 1 h at each temperature. A: amorphous and βs: β-spodumene.

curves, it is clear that about 38% weight loss for the sample LA2SIII (Fig. 4a) and about 35% weight loss for the sample LA4SIII were noticed (Fig. 4b) in the temperature region 30–300 °C. Another broad endothermic peak was appeared at around 525 °C for LA2SIII and LA4SIII (Fig. 4a and b) and a total weight loss of about 13 wt.% at the temperature region 300–600 °C occurred (Fig. 4a and b). There appeared the exothermic peaks at 790 °C for LA2SIII (Fig. 4a) and that at 785 °C for LA4SIII (Fig. 4b) accompanying practically no weight loss in the temperature region 600–1200 °C of the corresponding TG curves (Fig. 4a and b).

It is to be stated that the strong broad endothermic peaks appeared in the temperature range 140–150 °C for all the samples obtained from different sources were assigned to the removal of absorbed water and other volatiles present in the gel sample while the small endothermic peaks in the temperature region 250–270 °C of the same samples were attributed to the partial removal of structural hydroxyl groups and decomposition of nitrate ions [18] following their complete removal at around 485–530 °C showing another broad endothermic peak around the same temperature.

The exothermic peaks appeared at around 700 °C for the samples obtained from TEOS and fumed silica and that found at around 790 °C for rice husk source were due to the crystallization of eucryptite and/or spodumene. In the following Sections (Section 3.2), in studying XRD, it was confirmed that both the β-eucryptite and β-spodumene phases crystallized at 700 °C for TEOS and fumed silica sources and the same crystallized at 800 °C for rice husk ash source which supported the DTA results.

3.2. Crystallization behaviour of the gel powders by XRD

To study the crystallization behaviour of the phases appeared at different temperatures, XRD patterns of the gel powders are shown in Figs. 5a, b, 6a, b and 7a, b corresponding to the samples LA2SI, LA4SI, LA2SII, LA4SII, LA2SIII and LA4SIII, respectively, calcined at 400–1000 °C each. For the samples LA2SI and LA4SI obtained from TEOS, Fig. 5a and b, respectively, show that up to 600 °C, the samples remained amorphous. However, the crystallization of β-eucryptite and β-spodumene phases developed at 700 °C for the samples LA2SI and LA4SI, respectively, and the same retained up to 1000 °C for both the samples.

For the samples LA2SII and LA4SII, obtained from fumed silica, Fig. 6a and b, respectively, reveal that up to 600 °C, the crystallization did not occur. However, for the

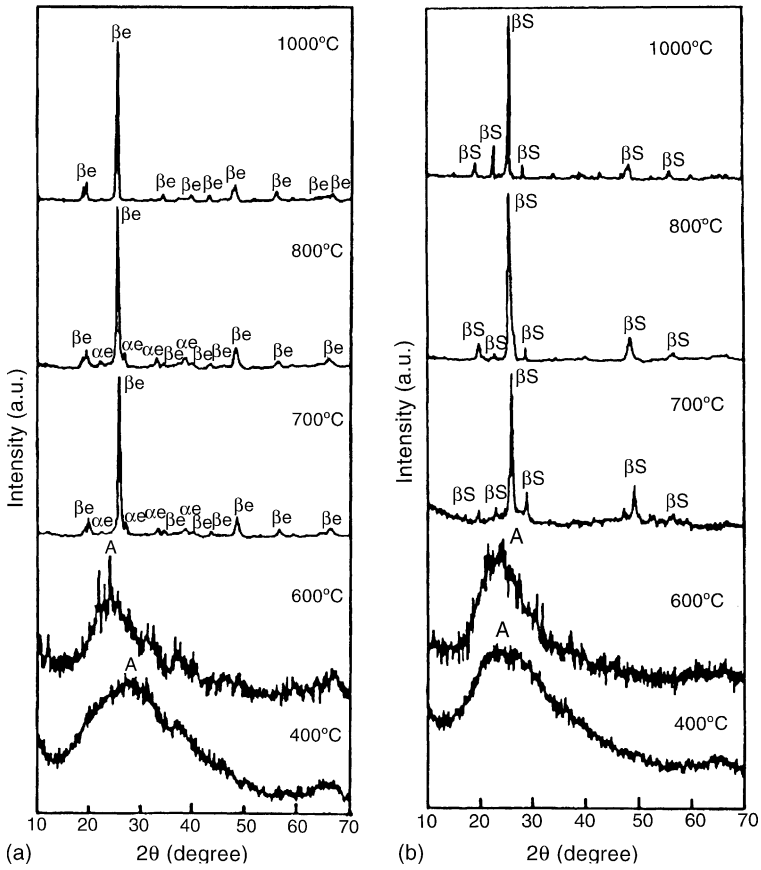

Fig. 6. (a) XRD patterns of LA2SII powders obtained from fumed silica and calcined at 400–1000 °C. *Note*: Dwell time: 1 h at each temperature. A: amorphous, αe: α-eucryptite and βe: β-eucryptite. (b) XRD patterns of LA4SII powders obtained from fumed silica and calcined at 400–1000 °C. *Note*: Dwell time: 1 h at each temperature. A: amorphous and βs: β-spodumene.

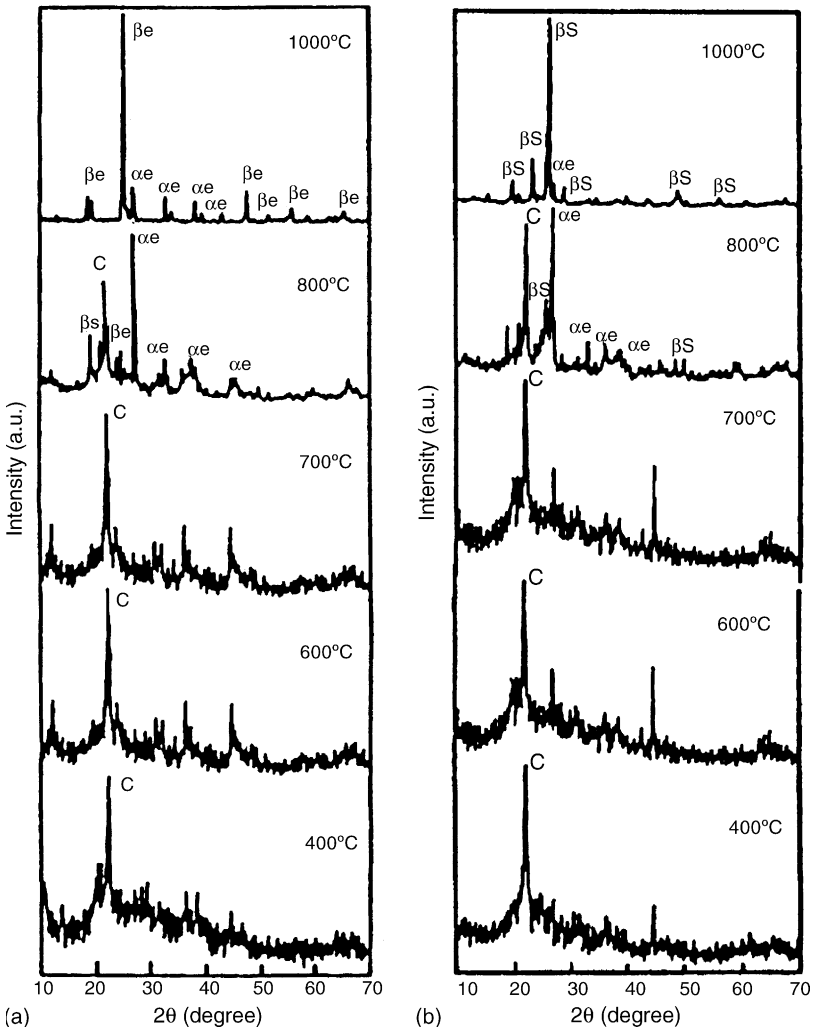

Fig. 7. (a) XRD patterns of LA2SIII powders obtained from rice husk ash and calcined at 400–1000 °C. *Note*: Dwell time: 1 h at each temperature. c: cristobalite, αe: α-eucryptite, βe: β-eucryptite and βs: β-spodumene. (b) XRD patterns of LA4SIII powders obtained from rice husk ash and calcined at 400–1000 °C. *Note*: Dwell time: 1 h at each temperature. c: cristobalite, αe: α-eucryptite and βs: β-spodumene.

sample LA2SII, β-eucryptite phase substantially developed with a very small amount of α-eucryptite phase at 700 °C and they persisted up to 800 °C followed by the complete transformation of β-eucryptite at 1000 °C. For the sample LA4SII, β-spodumene appeared as the only phase at 700 °C and it retained up to 1000 °C (Fig. 6b).

For the sample LA2SIII, Fig. 7a reveals that cristobalite phase was found at 400–800 °C. At 800 °C, a mix phase of α-eucryptite, β-eucryptite and β-spodumene appeared with cristobalite phase. A substantial increase of β-eucryptite phase was observed with further increase in temperature up to 1000 °C. For the sample LA4SIII, the cristobalite phase retained up to 800 °C with the crystallization of α-eucryptite and β-spodumene phases at the same temperature (Fig. 7b). The β-spodumene phase appeared in major quantity with a trace amount of α-eucryptite phase after heating the sample, LA4SIII at 1000 °C (Fig. 7b).

It is to be noted that with the use of TEOS as the source material of silica, a single phase of β-eucryptite for LA2SI (Fig. 5a) and another single phase of β-spodumene for LA4SI (Fig. 5b) were obtained at 700 °C. However, for fumed silica, β-eucryptite was substantially developed with a small amount of α-eucryptite at 700–800 °C for LA2SII (Fig. 6a) while the only phase of β-spodumene appeared at 700 °C for LA4SII (Fig. 6b). In case of rice husk ash as source materials, a mix phase of α-eucryptite, β-eucryptite, β-spodumene and cristobalite was obtained at 800 °C for LA2SIII (Fig. 7a) and another mix phase of β-spodumene, α-eucryptite and cristobalite was obtained at 800 °C for LA4SIII (Fig. 7b).

From the above observation, it is clear that the crystallization of β-eucryptite and/or β-spodumene occurred faster in case of TEOS and fumed silica followed by rice husk ash. Comparing the crystallization behaviour of TEOS and fumed silica sources, it is evident that the single phase, β-eucryptite appeared at 700 °C for the former (LA2SI in Fig. 5a) while the same was observed solely at 1000 °C for the latter (LA2SII in Fig. 6a). It can be pointed

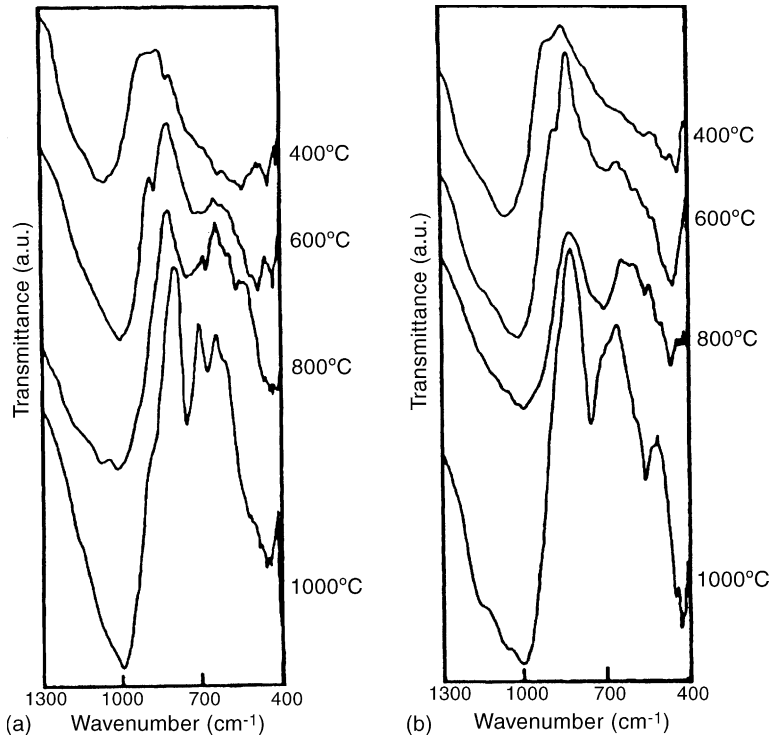

Fig. 8. FTIR spectra of (a) LA2SI powders and (b) LA4SI powders obtained from TEOS and calcined at 400–1000 °C.

out that the crystallization sequence of LAS powders with different sources of silica followed with the difference in the homogeneity of mixing of the constituents, lithia, alumina and silica. In the present case, a molecular level mixing occurred effecting better homogeneous reaction for TEOS source followed by fumed silica and rice husk ash sources where the particles are mixed as colloidal level and relatively larger level (−300 mesh size of rice husk ash),

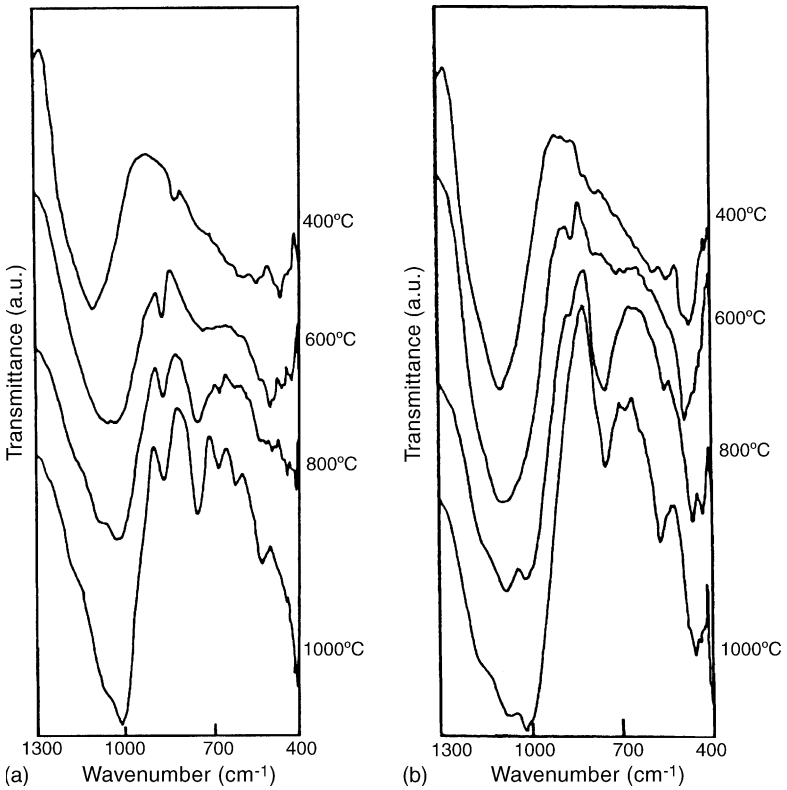

Fig. 9. FTIR spectra of (a) LA2SII powders and (b) LA4SII powders obtained from fumed silica and calcined at 400–1000 °C.

respectively. The above findings were also supported by the FTIR studies in the following section.

3.3. FTIR spectroscopy

To investigate the structural changes occurred towards the formation of lithium aluminum silicate through different phase transition of the powders calcined at 400 °C, 600 °C, 800 °C and 1000 °C, FTIR studies were performed in the wavenumber range 4000–400 cm^{-1}; however, the spectra in the wavenumber region 1300–400 cm^{-1} are presented for the samples LA2SI, LA4SI, LA2SII, LA4SII, LA2SIII and LA4SIII in Figs. 8a, b, 9a, b and 10a, b, respectively.

Figs. 8a–10b show that a strong broad band in the wavenumber region 1100–1000 cm^{-1} appeared in all the samples; however, the band shifted to higher wavelength region, i.e., towards 1000 cm^{-1} with increase in temperatures from 400 °C to 1000 °C. It indicated that more substitution of AlO_4 tetrahedra took place into SiO_4 tetrahedra unit [19]; therefore, the characteristics band for Si–O–Si vibration changed to Si–O–Al^{IV} vibration with increase in temperatures. A medium strong bands in the wavenumber region 800–950 cm^{-1} which are the characteristic absorption bands for AlO_6 octahedra [20,21] with nonbridging oxygens found to be present in the samples, LA2SI (Fig. 8a) and LA4SI (Fig. 8b) each calcined at 400–600 °C, LA2SII at 400–1000 °C (Fig. 9a), LA4SII at 400–600 °C (Fig. 9b), LA2SIII at 400–1000 °C (Fig. 10a) and LA4SIII at 400–800 °C (Fig. 10b) while there were no existence of such bands in the samples LA2SI (Fig. 8a) and LA4SI (Fig. 8b) each calcined at 800–1000 °C and LA4SII (Fig. 9b) and LA4SIII (Fig. 10b) each calcined at 1000 °C. It could indicate that at higher temperatures, AlO_6 octahedra changed to AlO_4 tetrahedra; and the latter enhanced the homogeneity of mixing [14] in LAS powders. In this case, TEOS silica source showed better homogeneity compared to fumed silica and rice husk ash sources.

A strong absorption band in the region 720–780 cm^{-1} appeared in the samples, LA2SI calcined at 800–1000 °C (Fig. 8a), LA4SI calcined at 1000 °C (Fig. 8b), LA2SII at 600–1000 °C (Fig. 9a), LA4SII at 800–1000 °C (Fig. 9b), LA2SIII at 600–1000 °C (Fig. 10a) and LA4SIII at 400–1000 °C (Fig. 10b) indicated the characteristic vibration of Al–O covalent bond in AlO_4 tetrahedra [3,19–24] in β-eucryptite (for LA2SI, LA2SII and LA2SIII) and in β-spodumene (for LA4SI, LA4SII and LA4SIII). An absorption band at around 670 cm^{-1} in LA2SI (Fig. 8a), LA2SII (Fig. 9a) and LA2SIII (Fig. 10a) each calcined at 800–1000 °C were also the characteristic band for β-eucryptite [21].

The absorption band observed at around 550 cm^{-1} for the sample LA4SI (Fig. 8b), LA4SII (Fig. 9b) and LA4SIII (Fig. 10b) each calcined at 800–1000 °C (Fig. 4b) was due to the presence of β-spodumene [24] assigning to the AlO_4 tetrahedra vibration [3]. At around 420–480 cm^{-1}, the absorption band found in all the spectra was the characteristic band of Si–O–Si bending vibration in SiO_4 tetrahedra [3,20,21].

From the above observation, it is to be noted that the characteristic absorption band at around 1005, 750, 670 and

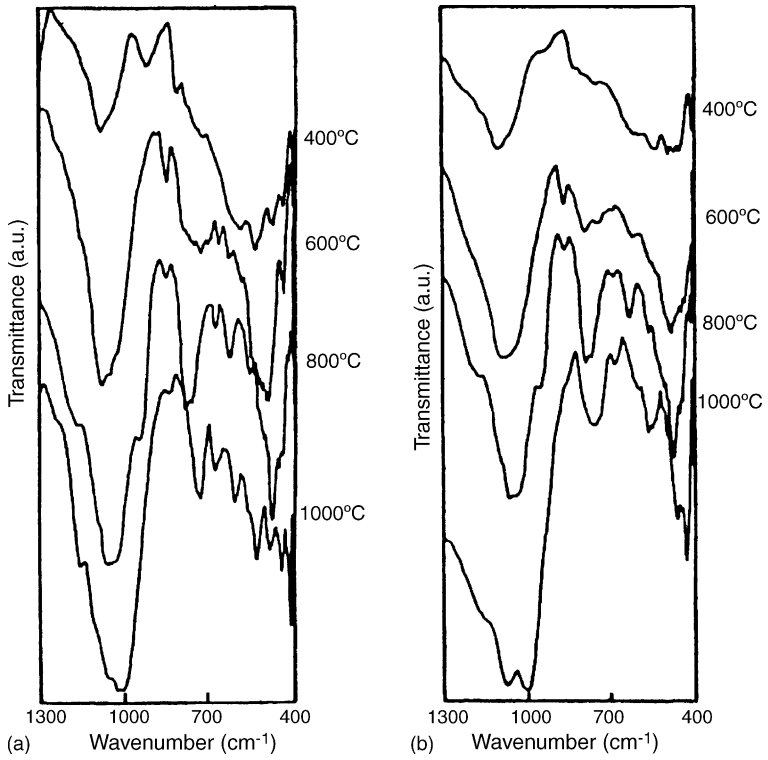

Fig. 10. FTIR spectra of (a) LA2SIII powders and (b) LA4SIII powders obtained from rice husk ash and calcined at 400–1000 °C.

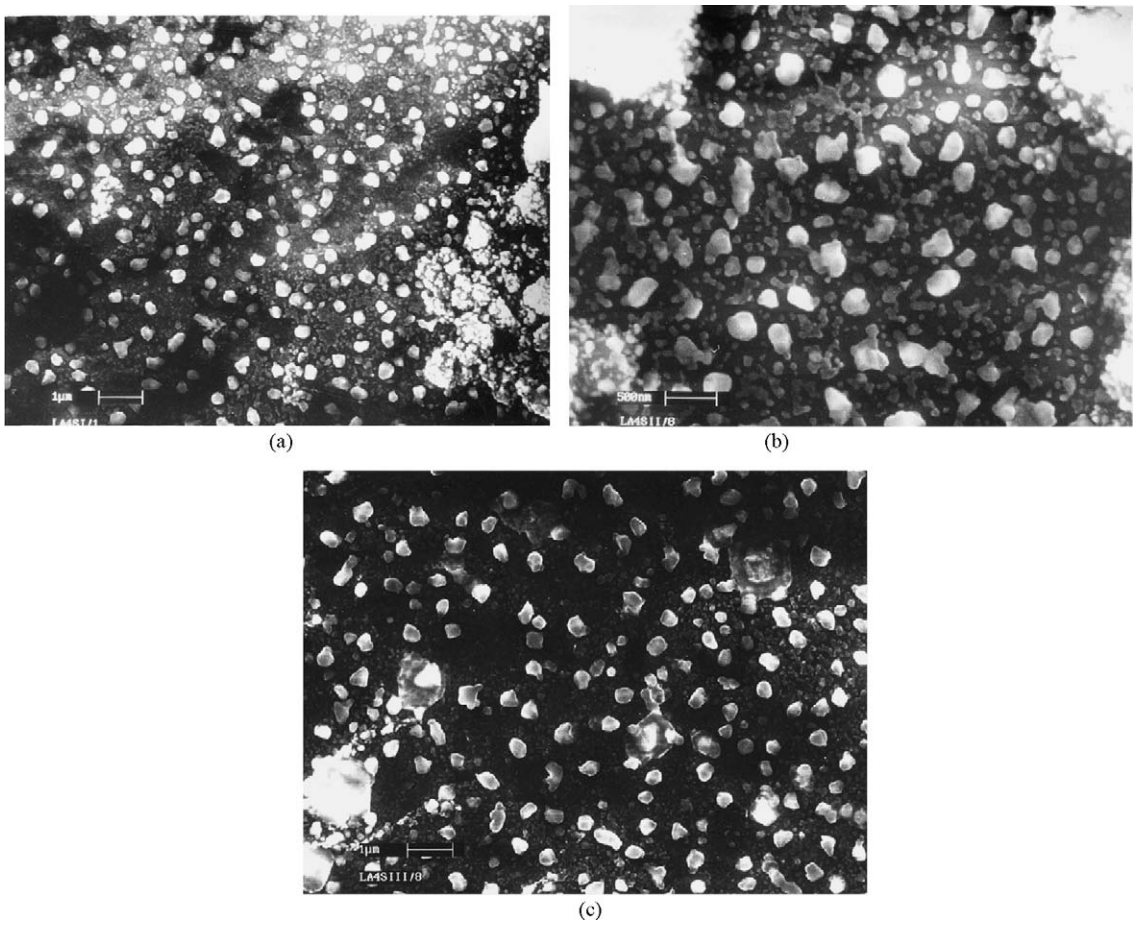

Fig. 11. SEM photograph of (a) LA4SI powders obtained from TEOS and calcined at 1000 °C; (b) LA4SII powders obtained from fumed silica and calcined at 1000 °C and (c) LA4SIII powders obtained from rice husk ash and calcined at 1000 °C.

445 cm^{-1} for LA2SI calcined at 800–1000 °C (Fig. 8a) was due to the presence of β-eucryptite [21]; however, for the sample LA2SII (Fig. 9a) and LA2SIII (Fig. 10a) calcined at 800–1000 °C each, in addition to the above absorption bands due to β-eucryptite, an additional band at around 865–850 cm^{-1} indicated the presence of nonbridging oxygens in AlO_6 octahedra. The characteristic absorption bands at around 1005, 750, 550 and 435 cm^{-1} for LA4SI calcined at 800–1000 °C (Fig. 8b) were assigned to the presence of β-spodumene [20,24]. FTIR results also confirmed a better homogeneity of mixing of alumina as AlO_4 tetrahedra in SiO_4 tetrahedra unit in LAS powders for TEOS silica source followed by fumed silica and rice husk ash sources. For the different phase transformations of LAS, the FTIR results corroborated the results obtained from XRD as discussed in Section 3.2.

3.4. Scanning electron microscopy (SEM)

Microstructural features of LAS powders obtained from different sources of silica, calcined at 1000 °C each are shown in Fig. 11a–c for LA4SI, LA4SII and LA4SIII, respectively. For the samples LA4SI, LA4SII and LA4SIII, Fig. 11a–c, respectively, reveal that the β-spodumene powders (as observed from XRD) were cobble-stone like morphology with particle size 100–300 nm. It is to be pointed out that there appeared no distinguishable morphology of β-spodumene for three different sources of silica. Similarly for β-eucryptite, no distinct features were observed (not shown in figures) for three different sources of silica.

4. Conclusions

(i) Lithium aluminum silicate (LAS) powders in the form of β-eucryptite and β-spodumene were synthesized by using different silica sources, i.e., TEOS, fumed silica and rice husk ash following sol–gel technique.
(ii) DTA and XRD results showed that crystallization of β-eucryptite and β-spodumene occurred faster with TEOS and fumed silica sources compared to rice husk ash silica source.
(iii) FTIR studies indicated that a more facile transformation of AlO_6 octahedra to AlO_4 tetrahedra occurred with TEOS silica source compared to fumed silica and rice husk ash.
(iv) XRD and FTIR studies confirmed that a better homogeneous reaction took place with the constituents,

Li_2O, Al_2O_3 and SiO_2 in LAS powders for TEOS silica source followed by fumed silica and rice husk ash sources.

(v) SEM indicated no distinguishable morphology of LAS powders for three different sources of silica.

Acknowledgements

The authors thank Dr. H.S. Maiti, Director of the Institute, for his kind permission to publish this paper. Thanks are also due to the members of the Technical Ceramics, SEM and X-ray Sections of the Institute for helping in characterization of the powders.

References

[1] A.I. Lichtenstein, R.O. Jones, S. De Gironcoli, S. Baroni, Anisotropic thermal expansion in silicates: a density functional study of β-eucryptite and related materials, Phys. Rev. B 62 (17) (2000) 11487–11493.

[2] B. Karmakar, P. Kundu, S. Jana, R.N. Dwivedi, Crystallization kinetics and mechanism of low expansion lithium alumino silicate glass-ceramics by dilatometry, J. Am. Ceram. Soc. 85 (10) (2002) 2572–2574.

[3] M.H. Lin, M.C. Wang, Crystallization behaviour of β-spodumene in the calcinations of Li_2O–Al_2O_3–SiO_2–ZrO_2 gels, J. Mater. Sci. 30 (10) (1995) 2716–2721.

[4] M.C. Wang, The effect of TiO_2 addition on the preparation and phase transformation for precursor β-spodumene powders, J. Mater. Res. 9 (1994) 2290–2297.

[5] B. Wang, S. Szu, M. Greenblatt, L. Klein, Ionic conductivity and structure of $(LiCl)_2$–Al_2O_3–SiO_2 xerogels, Chem. Mater. 4 (1992) 191–197.

[6] L. Zhien, S. Yihui, D. Xijiang, C. Jijian, Preparation and crystallization of ultrafine Li_2O–Al_2O_3–SiO_2 powders, J. Mater. Sci. 30 (2) (1995) 390–394.

[7] M.K. Naskar, M. Chatterjee, A novel process for the synthesis of lithium aluminum silicate powders from rice husk ash and other water-based precursor materials, Mater. Letts. 59 (8–9) (2005) 998–1003.

[8] M. K. Naskar, M. Chatterjee, A. Dey, A process of manufacturing lithium aluminosilicate powders, Ind. Patent, Application No. 1270/DEL/01 (2001).

[9] M.K. Naskar, M. Chatterjee, A novel process for the synthesis of cordierite ($Mg_2Al_4Si_5O_{18}$) powders from rice husk ash and other sources of silica and their comparative study, J. Eur. Ceram. Soc. 24 (13) (2004) 3499–3508.

[10] D.W. Johnson Jr., Sol–gel processing of ceramics and glass, Bull. Am. Ceram. Soc. 64 (12) (1985) 1597–1602.

[11] H. Dislich, Sol-Gel 1984–2004 (?), J. Non-Cryst. Solids 73 (3) (1985) 599–612.

[12] H. Schmidt, New type of non-crystalline solids between inorganic and organic materials, J. Non-Cryst. Solids 73 (3) (1985) 681–691.

[13] B. Samuneva, S. Jambazov, D. Lepkova, Y. Dimitriev, Sol–gel synthesis of $BaTiO_3$ and $Ba_{1-x-y}Ca_ySr_x(Zr_yTi_{1-y})O_3$ perovskite powders, Ceram. Int. 16 (6) (1990) 355–360.

[14] U. Selvaraj, S. Komarneni, R. Roy, Synthesis of glass-like cordierite from metal alkoxides and characterization by ^{27}Al and ^{29}Si MASNMR, J. Am. Ceram. Soc. 73 (12) (1990) 3663–3669.

[15] D.C. Bradley, R.C. Mehrotra, D.P. Gaur, Metal Alkoxides, Academic Press, NY, 1978.

[16] B.E. Yoldas, Monolithic glass formation by chemical polymerization, J. Mater. Sci. 14 (8) (1979) 1843–1849.

[17] H. Suzuki, K. Ota, H. Saito, Preparation of cordierite ceramics from metal alkoxides (Part 1), Yogyo-Kyokai-Shi (J. Ceram. Soc. Japan) 95 (2) (1987) 163–169.

[18] R. Petrovic, D. Janackovic, S. Zee, S. Drmanic, L. Kostic-Gvozdenovic, Phase-transformation kinetics in triphasic cordierite gel, J. Mater. Res. 16 (2) (2001) 451–458.

[19] M.K. Murthy, E.M. Kirby, Infrared study of compounds and solid solutions in the system lithia–alumina–silica, J. Am. Ceram. Soc. 45 (7) (1962) 324–329.

[20] L.A. Ignat'eva, Study of α- and β-spodumene by infrared spectroscopy, Opt. Spectrosc. 6 (6) (1959) 527–529.

[21] B.N. Roy, Spectroscopic analysis of the structure of silicate glasses along the joint $xMAlO_2$–$(1-x)SiO_2$ (M = Li, Na, K, Rb, Cs), J. Am. Ceram. Soc. 70 (3) (1987) 183.

[22] H.M. Jang, K.S. Kim, C.J. Jung, Chemical processing and densification characteristics of lithium aluminosilicate (LAS) gels, J. Mater. Res. 7 (8) (1992) 2273–2280.

[23] J. Covino, F.G.A. De Laat, R.A. Welsbie, Synthesis and preliminary processing of the sol-gel derived β-quartz lithium aluminum silicate, J. Non-Cryst. Solids 82 (3) (1986) 329–342.

[24] N.N. Ghosh, P. Pramanik, Aqueous sol–gel synthesis of spodumene and eucryptite powders, Br. Ceram. Trans. 96 (4) (1997) 155–159.